17 (2023) 100279

Contents lists available at ScienceDirect

International Journal of Thermofluids

journal homepage: www.sciencedirect.com/journal/international-journal-of-thermofluids

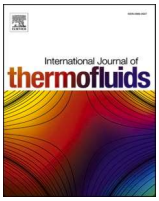

Numerical investigation on the performance of an innovative Airfoil-Bladed Savonius Hydrokinetic Turbine (ABSHKT) with deflector

Vimal N. Chaudhari [a,*], Samip P. Shah [b]

[a] Mechanical Engineering Department, Gujarat Technological University, Chandkheda, Ahmedabad, Gujarat 382424, India
[b] Mechanical Engineering Department, C.K.Pithawalla College of Engineering and Technology, Surat, Gujarat 395007, India

ARTICLE INFO

Keywords:
ABSHKT-Airfoil Bladed Savonius Hydrokinetic Turbine
SHKT-Savonius Hydrokinetic Turbine
TSR-Tip Speed Ratio, Ct-Coefficient of Torque
Cp-Coefficient of Power

ABSTRACT

Hydrokinetic energy has the least environmental impact and a high potential for small-scale energy production. Savonius hydrokinetic turbine extracts the hydrokinetic energy from the water current. It has a simple design and is inexpensive and quiet. The NACA6409 blades are implemented in place of conventional semi-circular blades of the Savonius hydrokinetic turbine and the newly Airfoil Bladed Savonius Hydrokinetic Turbine (ABSHKT) is developed. The deflector plate is implemented to enhance the performance of ABSHKT. A Computational Fluid Dynamics (CFD) simulation is conducted to analyze and compare the performance of ABSHKT with deflector to the conventional Savonius hydrokinetic turbine with deflector, with inlet velocity 1 m/s at various TSR range between 0.7 to 1.1. The present investigation shows that, the maximum power coefficient for ABSHKT and SHKT with deflector is 0.227 at 0.8 TSR and 0.25 at 0.8 TSR respectively. The ABSHKT with deflector has lower performance compared to SHKT with deflector. Implementing the enhanced augmentation technique is advisable to improve the performance of ABSHKT. The flow field spreading around the ABSHKT and SHKT with deflector is analyzed and discussed to compare the performance of both turbines with various aspects.

1. Introduction

The global need for energy is drastically increasing as the year passing. The need for energy globally increased by 5.8% in 2021 compared to 1.3% in 2019 and it continues to increase [1]. This need for energy is satisfied by energy generation from petroleum-based fuels and renewable energy sources. The energy produced from fossil fuels is the core reason for global warming besides of that the energy produced from renewable sources of energy is green energy. Because of that many agencies, research centers and governments are attracted to enhance renewable energy technologies. In global energy consumption, around 28% of energy is produced from renewable energy. From that, around 60% of renewable energy is produced from hydropower technology [2]. This is the remarkable contribution of hydropower technology to energy generation from renewable sources of energy. But the annual growth of energy produced from hydropower technology is degraded year by year so it needs to enhance the current hydropower technology [2].

The foremost advantages of hydropower technology are precise predictability, the least environmental impact and high energy density compared to wind energy [3]. Broadly, there are two approaches to utilizing hydropower energy. A huge hydropower station is developed with huge dams and a huge water reservoir to make a high head of water. It has a specific harmful impact on the environment such as loss of farmland, loss of forest and disturbing the aquatic lifecycle [4]. Besides that, the small-scale hydrokinetic energy resources available in the form of water currently available in the rivers and irrigation canals are a better opportunity to utilize hydrokinetic energy. Small-scale hydrokinetic energy has the least environmental impact and a promising for small-scale energy production [5]. The hydrokinetic energy is utilized with the help of the hydrokinetic turbine. The hydrokinetic turbines are also enabled to utilize the energy from the water currently available in outflows from industries, tidal current and any other water current. All the category of hydrokinetic kinetic turbine has some specific advantages such as a lower cost, independence from the flow direction and ease of maintenance as well as installation [6]. These all-hydrokinetic turbine blades are installed inside a framework that is coupled with a transmission system and generator to generate energy. The rotor axis of axial-flow hydrokinetic turbines rotates perpendicular to the flow of incoming water. While the cross-flow hydrokinetic turbine wita h vertical axihasve a vertical rotor axis to the flow of incoming water. Some of the famous hydrokinetic turbines with a vertical axis are the Savonius hydrokinetic turbine (SHKT) which has semi-circular blades, the Darrieus turbine which is a straight blade and the Gorlov turbine which has

* Corresponding author at: Government Polytechnic Waghai-Dang, Waghai, Ahwa Road, Rajendrapur, Ta - Waghai, Dist - Dang, Gujarat, 394730, India.
E-mail address: vimal4888@gmail.com (V.N. Chaudhari).

https://doi.org/10.1016/j.ijft.2023.100279

Available online 3 January 2023

Nomenclature

ABSHKT	Airfoil Bladed Savonius Hydrokinetic Turbine
SHKT	Savonius Hydrokinetic Turbine
TSR	Tip Speed Ratio
e	Gap or Overlap (mm)
d	Blade Diameter (mm)
D	Diameter of Turbine (mm)
De	Diameter of End Plate (mm)
H	Turbine Height (mm)
AR	Aspect Ratio
SWT	Savonius Wind Turbine
SST	Shear Stress Transport
k	Kinetic Energy of Turbulence
ω	Dissipation Specific Rate
MRF	Multiple Reference Frame
GGI	Generalized Grid Interface
URANS	Unsteady Reynolds Averaged Navier Stokes
C_t	Coefficient of Torque
C_{tmax}	Maximum Coefficient of Torque
C_p	Coefficient of Power
C_{pmax}	Maximum Coefficient of Power

helically shaped blades [7]. Among these, the SHKT has a simple design and is inexpensive and quiet. With good starting characteristics, it can receive fluid from any direction. Compared to a Darrieus-type turbine, it has a low aerodynamic efficiency [8].

The Savonius turbine's basic form is an "S" shape with a slight overlap between its two blades which has a semi-circular shape. One particular blade is referred to as the advancing blade which has a concave surface regarding the flow of water current and another blade is known as returning blade which has a convex surface regarding the flow of water current. Concave surfaces have a higher drag coefficient than convex surfaces which is exerted by the water current. Therefore, an advancing blade facing the water's current would experience additional drag compared to returning blade. The drag force differences among the concave and convex surface of the turbine blades, the blades start to rotate about a vertical shaft is the basis for the Savonius turbine's operation. This will produce the torque at the turbine's central shaft [8]. The turbine blades are secured by the end plates. These end plates also help to achieve a high-power coefficient and higher tip speed ratios [9]. As per Fig. 1, the SHKT is composed of two vertical half-cylinders. The letters "H", "D" and "De" stand for the turbine's height, turbine diameter and end plate diameter respectively. The geometrical parameters of SHKT are tabulated in Table 1.

The aspect ratio (AR) is the proportion of the height of the turbine to the diameter of the turbine. The overlap ratio (OR) is the proportion of the overlap (Gap) (e) to the blade diameter (d), which is another factor that influences the performance of SHKT. The advancing blade experiences the drag force from the water current while the returning blade experience the opposite force from the water current discharge from the gap which will a couple force that can produce torque. Regarding the principles of operation, SHKT and Savonius wind turbines (SWT) have many things in common. However, SHKT extracts considerable energy even at low speeds since water is 835 times denser than air [10]. In the past few years, numerous experimental, theoretical, and computational investigations on the SHKT have been conducted to enhance its performance. Similar to SWT, SHKT was equipped with various augmentation techniques to enhance performance, including various shaped deflectors, thick deflectors, arrangement of curtains, etc. According to published study findings from numerous authors, the design, operational and flow characteristics also have an impact on SHKT performance.

Numerous investigations were conducted on the SHKT to improve its performance by investigating the design of the blade profile [5,6,11–14, 15–18], the number of stages [19,20], aspect ratio and overlap ratio [21] and varieties of the technique of augmentation [22–26]. Alipour et al. [11] conducted a computational fluid dynamic study on parabolic blade shape SHKT particularly intended for small-scale power generation. In comparison to the arc shape trailed by a straight arc and a semicircular blade, the parabolic blade shape SHKT revealed gains in maximum power coefficient of 7.7% and 12%, respectively. Same way Talukdar et al. [12] conducted experiments on elliptical blades of two-bladed SHKT and found that the conventional two-bladed SHKT has greater performance correlated to elliptical blades of two-bladed SHKT. Singha et al. [13] analyze the performance of modified twisted-bladed SHKT. They analyze its performance at several operating conditions and several Tip Speed Ratio (TSR) and concluded that the Coefficient of Power (C_p) is remarkably higher compared to the previously most designed SHKT at all the TSR values. Wahyudi et al. [14] studied to select the most suitable tandem blade SHKT out of three designed models and find the ideal tandem radius blade clearance to optimize the performance of the designed model. Anuj Kumar et al. [6] have worked on two geometrical factors as shape factor of the blade and the arc angle of the blade. These two factors have been taken into account to change the blade shape of the SHKT. According to their experiment, the arc angle of the blade is 15° and the shape factor of the blade is 0.6, which corresponds to a 0.9 TSR at a 2 m/s flow velocity, resulting in a maximum power coefficient value of 0.426. Zhang et al. [16] have altered the design of SHKT with rotor angle and altered the rotor geometry by blade shape factor. They have refined and analyzed the modified SHKT employing the computational fluid dynamics methods and also observed that the blade shape factor how well affects the performance of the modified SHKT. Mosbahi et al. [15] experimentally investigated the parameters, which affect the performance of a twisted blade SHKT in a manmade canal. They have developed three designs of deflectors and examined them numerically to increase the effectiveness of the twisted blade SHKT. They found that the highest C_p was raised by 17.48% with the deflector. Shashikumar et al. [17] have conducted the computational fluid dynamics simulation by utilizing the ANSYS-fluent to examine the performance of conventional SHKT and the tapered blade SHKT to utilize the hydrokinetic energy from the water current. They observed that the performance of the tapered blade SHKT with a 5° taper angle was lowered by 5% compared to the conventional SHKT. Patel et al. [18] have designed the two innovative SHKT blades and conducted an experimental analysis to observe the performance of the same with convention SHKT. They observed that the extended semi-cylindrical blade performs well respected to the remaining design. Basumatary et al. [5] first time developed a new collective lift and drag force base design of blade for a conventional 2-bladed SHKT and conducted a numerical analysis. They changed the conventional semi-circular blade with the airfoil blade section at the leading edge at the end of the blade and the straight blade section near the central axis of the turbine. When run under the same design parameters and operational conditions as the standard SHKT design, the new collective lift and drag force base design of the blade for a conventional 2-bladed SHKT shows greater performance. Further, Basumatary et al. [27] have conducted an experimental analysis on the new collective lift and drag force base design of the blade for a conventional 2-bladed SHKT, which was already numerically investigated by Basumatary et al. [5]. Again, they found that the new collective lift and drag force base design of the blade for a conventional 2-bladed SHKT shows greater performance compared to the standard SHKT design. Khan et al. [28] implemented the new blade design as the section of S1048 airfoil blades in place of conventional SHKT semi-circular blades. The section of blades was composed of straight and curved sections of the S1048 airfoil blade. They observed that the highest C_p of the new blade design was 14% higher than the conventional SHKT.

Prabowoputra et al. [19] have worked on the influence of some

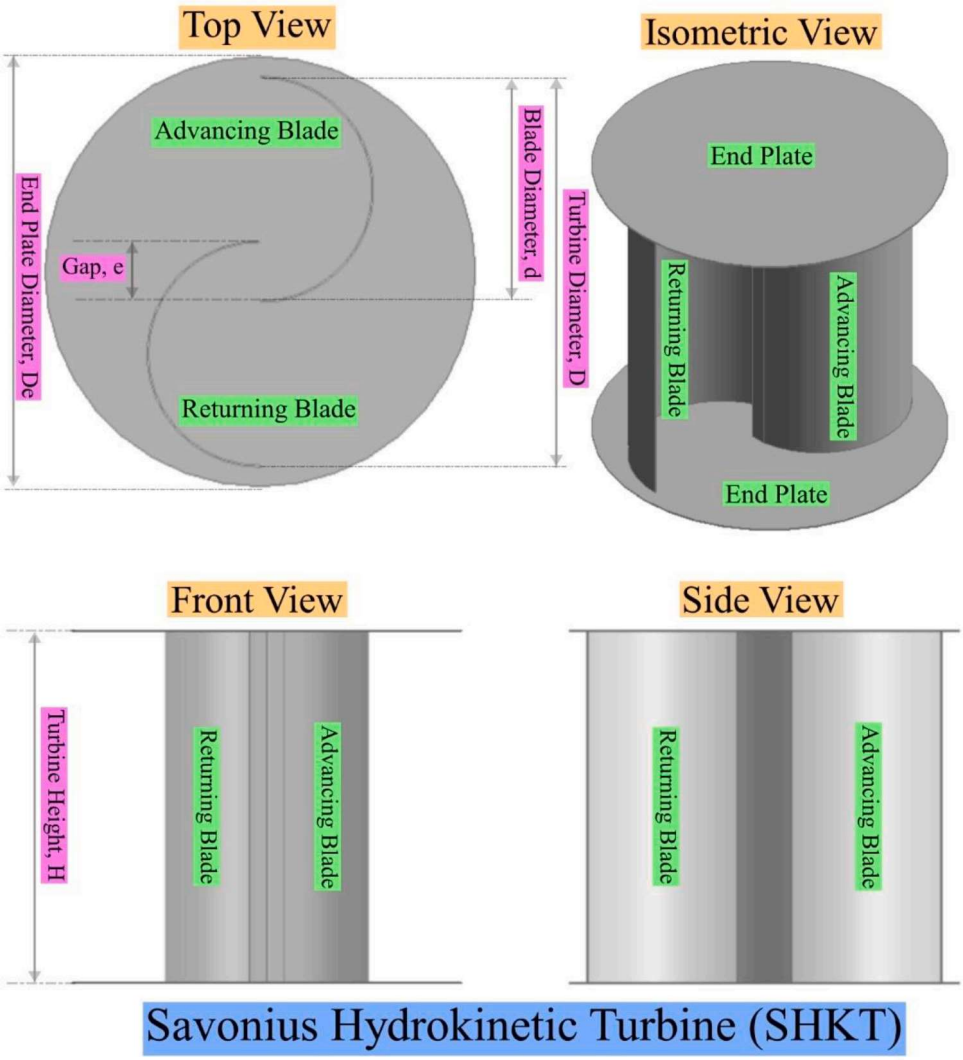

Fig. 1. Design of 2-Bladed Savonius Hydrokinetic Turbine (SHKT).

Table 1
Geometrical parameters of SHKT and ABSHKT.

Sr. No.	Geometrical Parameters	SHKT	ABSHKT
1.	Diameter of blade (mm), d	144	144
2.	Diameter of the turbine (mm), D	250	250
3.	Height of turbine (mm), H	250	250
4.	Gap (mm), e	38	38
5.	End plate diameter (mm), De	277.2	277.2
6.	End plate thickness (mm)	1	1
7.	Turbine blade thickness (mm)	1	Varying
8.	Aspect Ratio, AR	1	1

stages on the performance of SHKT. They concluded that the maximum average torque and performance of the two-stage SHKT were higher compared to another design concerning the number of stages. Anuj Kumar et al. [20] have also worked on twisted blade SHKT with a different number of stages. They also concluded that the maximum average torque and performance of the two-stage SHKT was higher compared to another design concerned with the number of stages.

Patel et al. [21] have studied the impact of the aspect ratio and overlap ratio on the performance of the SHKT to generate hydrokinetic energy from the water current. They observed that the performance of the SHKT was increased as the aspect ratio increased for the fixed overlap ratio but still the performance improvement is stable as the aspect ratio is higher than 1.8.

A significant reason for the degraded performance of the SHKT is the negative torque generated by the returning blade. So Alizadeh et al. [22] have tried to improve the performance by diverting water current from the returning by employing the simple deflector. The computational fluid dynamics study was conducted to analyze the impact of deflector length and they concluded that the optimized length of the deflector can improve the performance by 18% compared to simple conventional SHKT. Golecha et al. [23] have worked on the ideal placement of the deflector, upstream to the water current, to improve the performance of the modified SHKT. They experimented on eight different positions of the deflector to observe the effect of the deflector position on the performance of the SHKT. Wahyudi et al. [24] also implement the deflector to enhance the performance of the tandem blade SHKT. They implement the radial moving plate deflector and tangential moving plate deflector. They observed that the tandem blade SHKT with tangential moving plate deflector performs well compared to the turbine with radial moving plate deflector. Kerikous et al. [25] have also worked on deflector plates. They have worked on the optimization of the position and shape of the thick deflector plate. They concluded that the thick deflector plate can protect the returning blade from the impact of the water current which is responsible for the negative torque production so the implementation of the thick deflector plate can enhance the performance of the SHKT. Thakur et al. [26] presented an intruding jet duct

design to enhance the performance of SHKT. It was observed that the current design of SHKT performs better than the conventional SHKT. Based on the above investigation there is more scope in the design of the SHKT blade profile and augmentation technique to improve the performance of SHKT.

Savonius hydrokinetic turbine has important benefits, like simplicity in design, inexpensive, quiet operation and good starting characteristics [8]. Because of that much research has been conducted on the SHKT to improve its performance compared to conventional SHKT. Among the previous investigation on the blade design, the elliptical blade SHKT [12] and tapered blade SHKT [17] has performed low compared to the conventional SHKT. They examine that the negative torque generation in the returning blade was the significant cause for the decrement in the performance of the new design SHKT compared to conventional SHKT. This motivates the present author to develop a new design of the SHKT blade to improve its performance compared to conventional SHKT. Besides that, the previous investigation on the blade design of SHKT, parabolic blade shape SHKT [11], modified twisted-bladed SHKT [13], modified angle of arc and shape factor of the blade of SHKT [6], extended semi-cylindrical blade [18] and a new collective lift and drag force bases design of blade [5] have improved performance compared to convention SHKT for the same geometry and operational criteria. The performance improvement observed by the new collective lift and drag force base design of the blade is a significant motivation for the current investigation. They observed that greater velocity spreading near the advancing blade and returning blade are the core reason for the performance improvement. The curve section of the airfoil leading edge is a reason for the higher velocity distribution [5]. The investigation conducted on airfoil blades concluded that the drag-based airfoil blade is aerodynamically less efficient compared to the lift-based airfoil blade profile [29–31]. It is observed that the lift force is useful to improve the performance of the SHKT so the idea is generated by the present author to implement the full airfoil blade in place of the conventional semi-circular blades of SHKT. The implementation of the full airfoil blade to the SHKT is still not analyzed in any previous investigation by the other authors. Basumatary et al. [5] and Basumatary et al. [27] have replaced the conventional semi-circular blades of SHKT by combining a straight blade section and a curve section of NACA0018 airfoil. Their purpose is to improve the performance of the turbine by covering more surface area of the blade with incoming water current to extract much more energy from the water current. Khan et al. [28] have replaced the conventional semi-circular blades of SHKT with straight and curved sections of the S1048 airfoil blade. Their purpose is to improve the performance of the turbine by increasing the moment arm with a long straight edge and to decrease negative torque by curve section. The above investigations [5,27] and [28] are conducted on the implementation of a section of airfoil blades only but the present investigation is conducted to analyze the performance of full NACA6409 9% airfoil blades, with chord 158.7 mm, radius 105 mm and thickness 100%, in place of a conventional blade of SHKT. The selection of full NACA6409 is based on the geometrical similarities with the conventional design of SHKT and the compatibility of the NACA blade for the installation as a blade in SHKT. In the present investigation, it is expected to improve the performance of NACA6409 bladed SHKT by an effective generation of lift force at some specific angle of rotation of the turbine. It is observed from the previous investigation, the augmentation technique works very effectively to improve the performance of SHKT. The deflector plates are very compatible as an augmentation technique because of their simple design, liberty in position respected to SHKT and cost [22–26]. This is a motivation for the present author to implement the deflector plate for performance improvement. So, the present investigation also works on the influence of the deflector plate on the performance of conventional SHKT and the newly designed Airfoil Bladed Savonius Hydrokinetic Turbine (ABSHKT).

To study the influence of the airfoil blade and the deflector plate, the transient 3D CFD simulation is conducted on SHKT. The objectives of the present investigation are as follows.

1 To study the effect of deflector plates on the performance of conventional SHKT and the newly designed Airfoil Bladed Savonius Hydrokinetic Turbine (ABSHKT).
2 To study and compare the performance, in terms of torque coefficient and power coefficient, of conventional SHKT and ABSHKT with deflector plate.
3 To study the pressure distribution and velocity distribution for the conventional SHKT and ABSHKT, with deflector plate, for the various TSR.

2. Introduction to the design of 2-bladed conventional SHKT and ABSHKT

The diagram of the SHKT is shown in Fig. 1, which is developed using ANSYS DesignModeler. The dimensional parameters of the SHKT are tabulated in Table 1.

The SHKT is composed of two vertical semi-circular blades. One blade is known as the advancing blade which has a concave surface relating to the direction of the water current and another blade is known as returning blade which has a concave surface relating to the direction of the water current. The geometrical parameters of the SHKT and ABSHKT such as the diameter of the turbine blade, the turbine diameter which is constant through the height, the height of the turbine including the end plate, Gap is also known as overlap, end plate diameter is similar for both top end plate and bottom end plate, Thickness of turbine blade is constant for SHKT and Aspect ratio is similar as Talukdar et al. [12].

The geometrical parameters of ABSHKT are identical to the SHKT. The ABSHKT consists of NACA6409 9% blades in place of conventional semi-circular blades of SHKT with chord 158.7 mm, radius 105 mm and thickness 100% blade (Fig. 2) in place of a conventional blade of SHKT as shown in Fig. 3. The selection of NACA6409 is based on the geometrical similarities with the conventional design of SHKT and the compatibility of the NACA blade for the installation as a blade in SHKT. The thickness of the blade of ABSHKT is varying as per the blade profile. The deflector plate is placed upstream of ABSHKT as shown in Fig. 4.

3. Numerical analysis procedure

3.1. Computational domain and boundary conditions

Computational Fluid Dynamics (CFD) analysis is a very effective tool for the analysis of the fluid flow problem so, in the present investigation, this is used to analyze the performance of SHKT and ABSHKT. The configuration of the computational domain and the boundary conditions are maintained similarly for both SHKT and ABSHKT. The Ansys-DesignModeler is used to generate a 3D model of SHKT and ABSHKT. The design parameters of both models are mentioned in Table 1. If the turbine model is symmetrical along the vertical axis, then the 2D model is sufficient for the numerical analysis [32].

Both turbine models are offered with end plates, so the 3D model is preferred for the present numerical analysis. The domain has mainly two different volumes as shown in Fig. 5. The turbine is confined into the cylindrical volume which is the rotating zone and this cylindrical volume is confined into the rectangular cubic stationary volume which is the stationary zone. During the numerical analysis, the cylindrical volume is rotated about Y-axis at a required TSR. Each volume is interconnected by the interface. The interface plays a significant role in the continuity of the incoming flow to the rotating zone from the stationary zone. The diameter of the cylindrical volume is 310 mm, which is almost 1.2D compared to the diameter of a turbine blade (D), and the height is 400 mm. The dimension of the cubic volume is quantified as 2500 mm length x 1500 mm width x 750 mm height is about 10D x 6D x 3D [12].

The boundary defined for the present numerical analysis is mentioned in Fig. 5 and also in the tabulated form as per Table 2. The

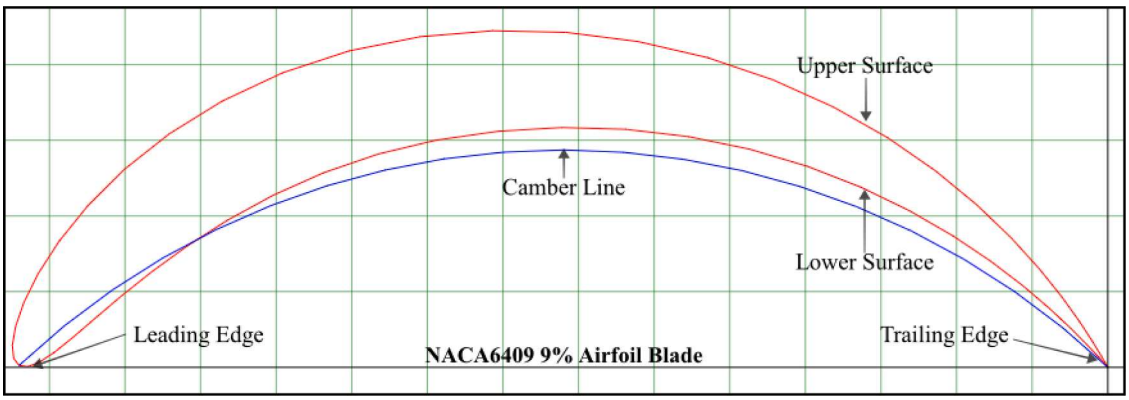

Fig. 2. Design of NACA6409 9%.

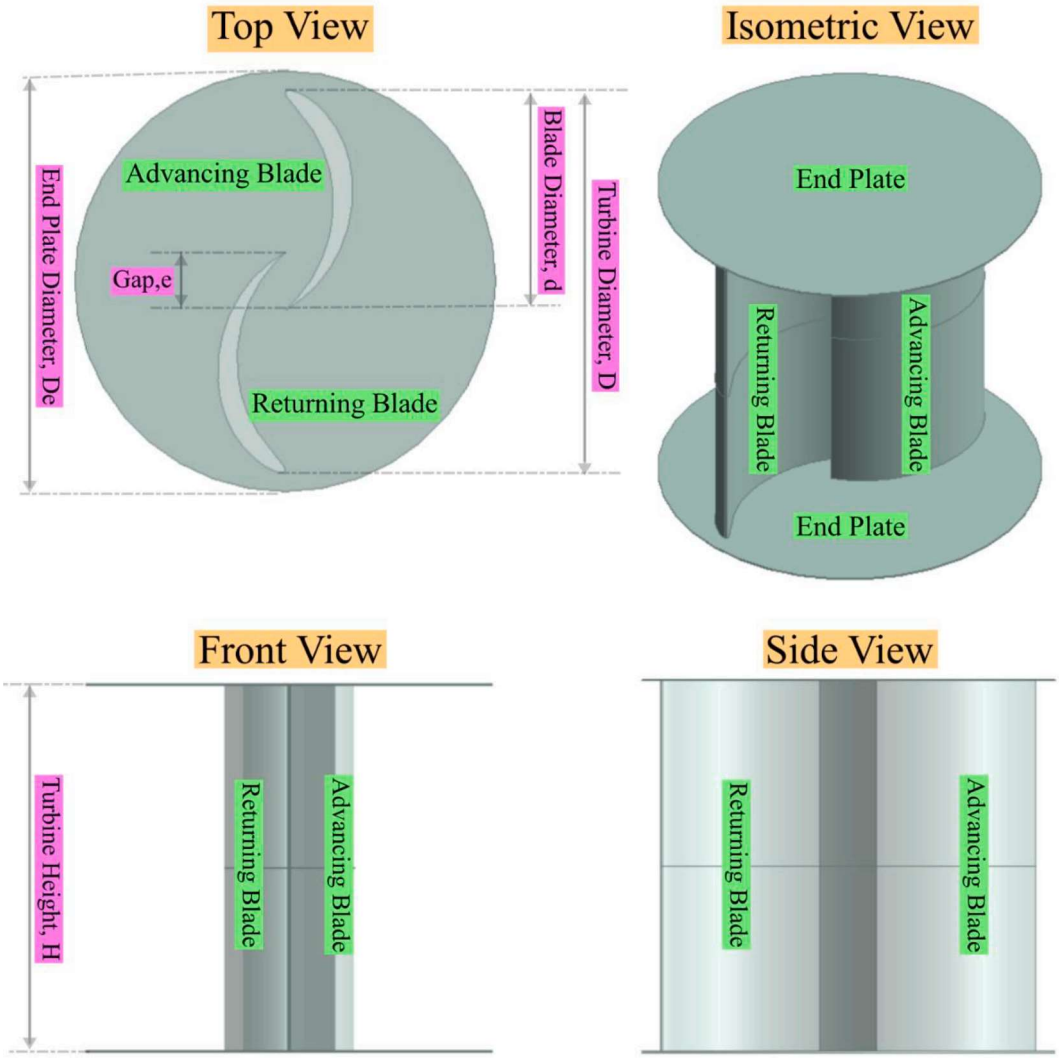

Fig. 3. Design of Airfoil Bladed Savonius Hydrokinetic Turbine (ABSHKT).

velocity inlet boundary condition is specified for the left side plane of the stationary zone and always uniform velocity inlet is maintained for all the values of TSR. The right-side plane of the stationary zone is stated as an outflow boundary condition with 1atm pressure outflow [33, 34]. The remaining four side planes are specified as symmetry boundary conditions because the practical fluid flow channel has a higher value of dimension compared to the simulated domain dimension. The turbine is assigned as the rotating wall condition with no slip wall criteria. The top and bottom faces of a rotating zone are specified as the symmetry boundary condition. The specified boundary condition in the present study is the most effective boundary condition for analysis of the 3D simulation performance of the turbine in numerous investigations [6,11, 12].

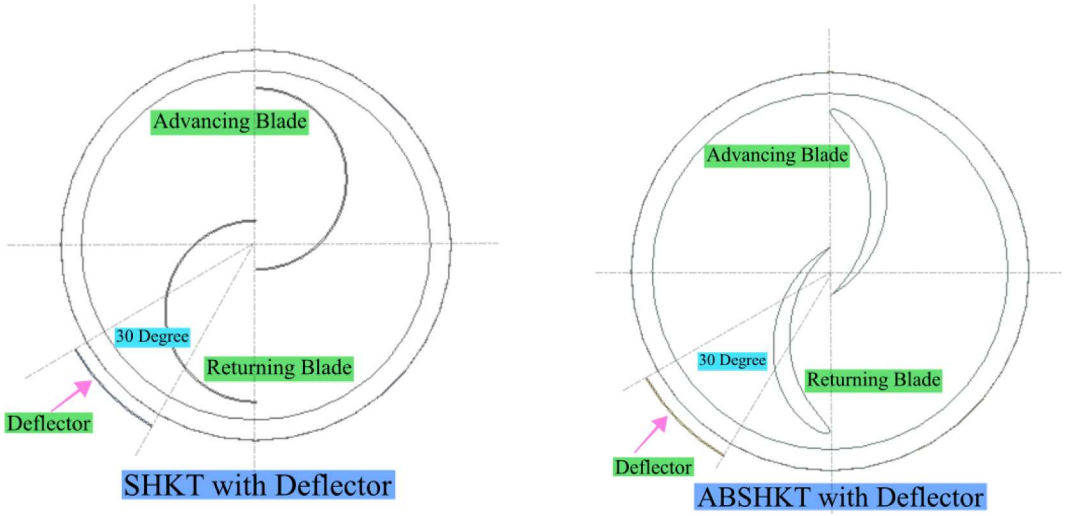

Fig. 4. SHKT and ABSHKT with Deflector.

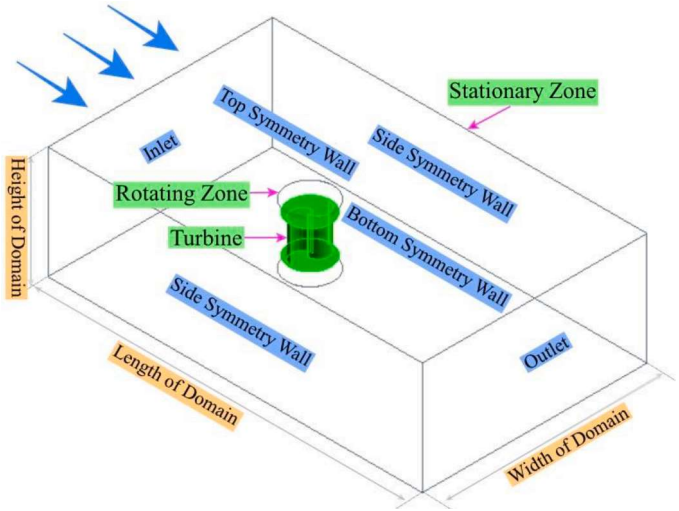

Fig. 5. Isometric view of the computational domain.

Table 2
Boundary condition applied to both SHKT and ABSHKT simulation.

Sr. No.	Name	Type of Boundary	Boundary conditions
1.	Inlet	Velocity inlet	1 m/s
2.	Outlet	Pressure opening	1 atm
3.	Sides, top and bottom wall	Symmetry	Symmetry
4.	Turbine	No-slip wall	The rotating zone with the turbine has angular velocity as per TSR (0.7–1.2)

3.2. Grid generation

In the current investigation, the grid is generated by the ANSYS MESH for the 3D model of both the turbine. The grid is generated with the tetrahedral elements having a non-conformal unstructured grid for the entire water current domain as shown in Fig. 6.

The fine mesh is created at the rotating zone related to the mesh generated in the stationary zone, to conduct a details study of turbulence generated near the turbine. The wall of the turbine experienced a high-pressure gradient during the rotation. To capture this high-pressure gradient and flow near the wall, the inflation layer is set at the turbine wall having a total thickness of 12 numbers of layers and a maximum thickness of 0.005. To conduct the grid independence test, three different numbers of mesh elements in the range 7,630,000 to 655,000 are studied for the entire water current domain. It is observed that, for all three different meshing conditions, there is negligible change in the C_p generated by the SHKT so it is advisable to conduct a simulation with 1,175,092 numbers of mesh elements for SHKT in the present investigation. The grid generation for the other turbine simulation of ABSHKT, SHKT and ABSHKT with and without deflector plates, are conducted with the identical grid generation parameters as above.

3.3. Simulation procedure

Based on the previous investigation the CFD is an efficient tool to study fluid flow problem analysis. The present investigation is using this tool as an Ansys-CFX 2020R to analyze the performance of the turbine. For the simulation, numerous turbulence models are available. The selection of the turbulence model is a crucial task for precise simulation. Several numbers of turbulence models are existing to watch over the various factor that affects the simulation of a turbine. Among this, the Shear Stress Transport (SST) k-ω turbulence is used for the present investigation. The key advantage of the k-ω model is a development of a boundary layer at the turbine and the key advantage of the k-ε model is the development of free stream flow. The SST k-ω turbulence model has merged the advantages of both these models. High precision at the boundary layer is necessary for the turbine for the present investigation, this is fulfilled by the SST k-ω turbulence model also it is effective through the flow field [35,36]. The rotating zone is equipped with a Multiple Reference Frame (MRF) to solve an equation in a rotational reference frame [37]. The interface is set up between the rotating zone and the stationary zone with a Generalized Grid Interface (GGI) to secure the rotation of the turbine. This SST k-ω turbulence model is equipped with Unsteady Reynolds Averaged Navier Stokes (URANS) model for the algorithm computation.

The time step plays a significant role in the transient simulation of a turbine. The large time step would be the reason for the unlikely result of the simulation [6]. In the present investigation, it is advisable to make the time step as 1° rotation for the turbine same as the other investigation and also it is advisable to make the time step as per the TSR value [11,12]. So, the torque can be found at each degree of rotation and the magnitude error could be reduced. The total number of convergence criteria is set to 25 for the quasi-steady state attainment.

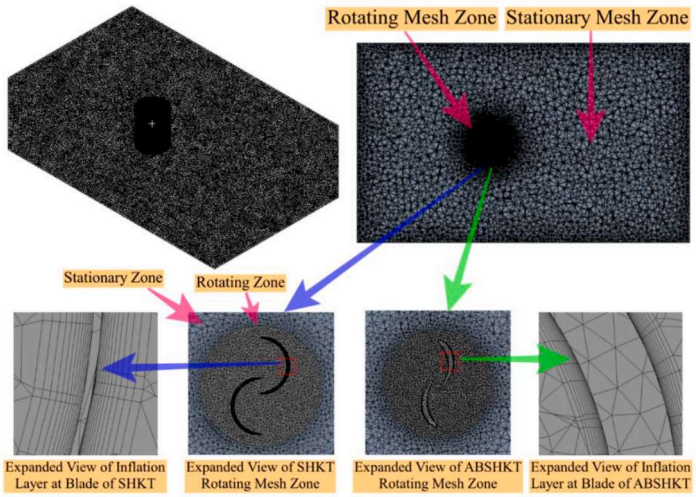

Fig. 6. Meshing of the computational domain for SHKT and ABSHKT.

4. Data reduction

The performance comparison of ABSHKT with and without deflector with the conventional SHKT is analyzed by obtaining performance parameters that are Power Coefficient (C_p) and the Torque Coefficient (C_t) at different TSR. To get the value of performance parameters from simulation, the torque produced can be obtained from the result of simulation at different Tip Speed Ratio. The performance parameters are stated as following equations:

$$TSR = \frac{\omega R}{V} \tag{1}$$

$$C_t = \frac{T}{0.5\rho A V^2 R} \tag{2}$$

$$C_p = \frac{P_{in}}{P_{out}} = \frac{T\omega}{0.5\rho A V^2 R} = \frac{C_t \omega R}{V} = (C_t)(TSR) \tag{3}$$

$$A = DH. \tag{4}$$

Where,

ω = Angular Velocity (rad/*sec*) R = Radius of the turbine (m)

V = Inlet velocity (m/s) P_{in} = Power generated by a turbine

P_{out} = Hydraulic energy in the water current ρ = Water density (kg/m^3)

A = Turbine swept area (m^2) H and D = Height and Diameter of the turbine

In the present investigation, the inlet velocity is kept always constant at 1 m/s for all the cases, so the Reynolds number is considered as follows.

$$Re = \frac{\rho V D}{\mu}$$

Where,

ρ = Density of water = 998 kg/m^3 V = Inlet velocity = 1 m/s

D = Diameter of turbine = 0.250 m μ = Dynamic viscosity of the water = 0.001 kg/ms^{-1}

Based on the above calculation, the Reynolds number (*Re*) is 2.5 × 10^5 used for the present investigation. The result generated from the present investigation is validated by Talukdar et al. [12]. The design parameters of SHKT and ABSHKT without deflector are kept identical to the SHKT without deflector studied in the reference paper. The present investigation is conducted at Reynolds number 2.25 × 10^5 identical to the reference paper. The validation is conducted with an inlet velocity of 0.8 m/s and the TSR 0.89. Fig. 7 shows the variation of C_p concerning various TSR of the present investigation of SHKT without deflector and the result produced by Talukdar et al. [12] for validation purpose. The value of C_p generated by the present investigation show (Fig. 7) the identical behavior as the C_p generated by 2D simulation and experiment conducted by Talukdar et al. [12]. So, it is illustrating that the flow behavior has been appropriately arrested by the present simulation procedure.

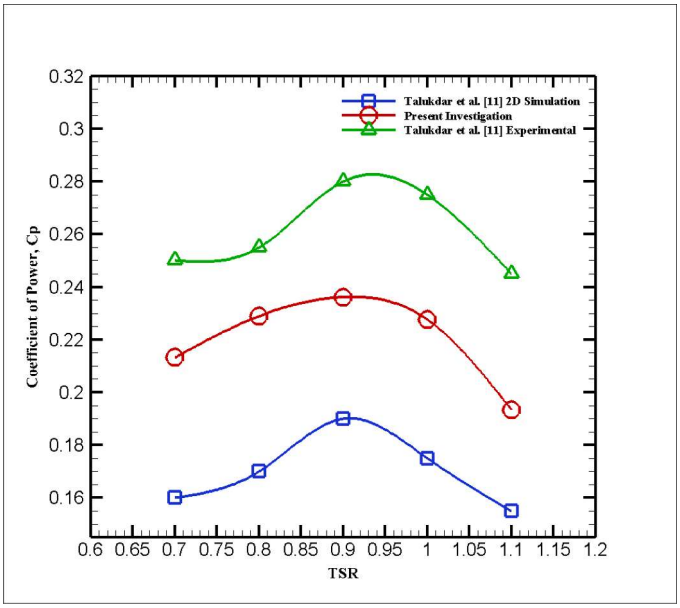

Fig. 7. Validation of simulation procedure with Talukdar et al., 2018, [12].

5. Result and discussion

The present investigation is conducted to analyze the performance of the NACA6409 9% blade in place of a conventional blade of SHKT. The 3D models for the various setup of Savonius Hydrokinetic Turbines are developed for the simulation using the tool Ansys-CFX 2020R. Usually, Savonius Hydrokinetic Turbines are available with conventional semi-circular blades. From the previous investigation, not a single investigation was conducted on the implementation of full Airfoil blades in place of conventional semi-circular blades of SHKT. So, a new turbine Airfoil Bladed Savonius Hydrokinetic Turbine (ABSHKT) is developed with NACA6409 9% blades and the performance is compared with the

conventional SHKT. Initially, the numerical analysis is conducted on the ABSHKT without deflector and SHKT without deflector to compare the performance by C_p and C_t generated by the inlet velocity 0.8 m/s and the TSR 0.9 and the flow physics around the turbine is examined with pressure contour and velocity contour at the various angle of rotation 0°, 30°, 60°, 90°, 120° and 150° of the SHKT and ABSHKT without deflector. The average C_t generated by the ABSHKT and SHKT without deflector are 0.24 and 0.29 respectively and the average C_p generated are 0.19 and 0.23 respectively at inlet velocity 0.8 m/s and the TSR 0.9. As shown in Fig. 8, the C_t of ABSHKT without deflector is highest at 0.602 at 32° and 212° of rotational angle compared to the highest C_t = 0.534 of SHKT without deflector at 20° and 200° of rotational angle because the lift force is generated in the airfoil blades of ABSHKT without deflector. Fig. 9 is plotted only for 0° to 90° of the rotational angle of a turbine to compare the generation of lift force produced in ABSHKT and SHKT without deflector. As shown in Fig. 9, the higher lift force is generated in ABSHKT without a deflector because of the airfoil section of blades compared to the SHKT without deflector. Besides that, the higher-pressure range is observed (Fig. 10) on the convex side of returning blades, at 120° of rotational angle, for ABSHKT without deflector compared to the convex side of returning blades of SHKT without deflector. Because of that, the negative C_t = 0.155 generated by ABSHKT without deflector (Fig. 8) at rotational angles 116° and 296° are very lower compared to the C_t generated by SHKT without deflector. So, it is observed the overall performance of ABSHKT without a deflector is lower compared to SHKT without a deflector but for a specific range of degrees of the rotational angle of the turbine, the torque generation is higher to ABSHKT without a deflector compared to the SHKT without deflector. The negative torque generation, generated by the returning blade of ABSHKT without deflector, is very much higher compared to the negative torque generated on the returning blade of SHKT without deflector could be the possible reason behind the lower performance of ABSHKT without deflector compared to SHKT without deflector. So, the deflector plate is implemented to decrease the effect of negative torque generated in ABSHKT without deflector as shown in Fig. 4. So the further investigation is conducted on ABSHKT and SHKT with deflector plate to examine the performance concerning C_p and C_t, with the inlet velocity 1 m/s and the TSR in the range of 0.7 to 1.1 by the increment of 0.1 in TSR.

Figs. 11 and 12 show the graph of C_t vs TSR and C_p vs TSR. It is observed that, the C_{tmax} and C_{pmax} for the ABSHKT with deflector are 0.324 and 0.227 at a TSR 0.7 and TSR 0.8 respectively. And for the SHKT

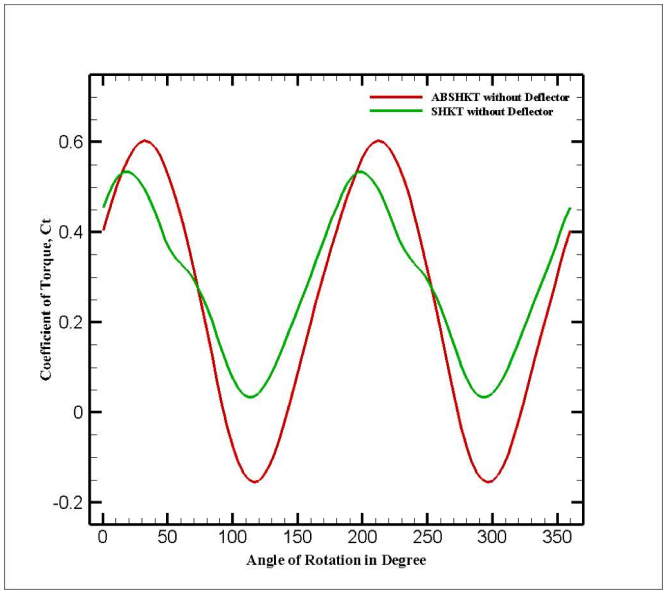

Fig. 8. Changes in Coefficient of Torque (C_t) about Angle of Rotation for the SHKT without Deflector and ABSHKT without Deflector.

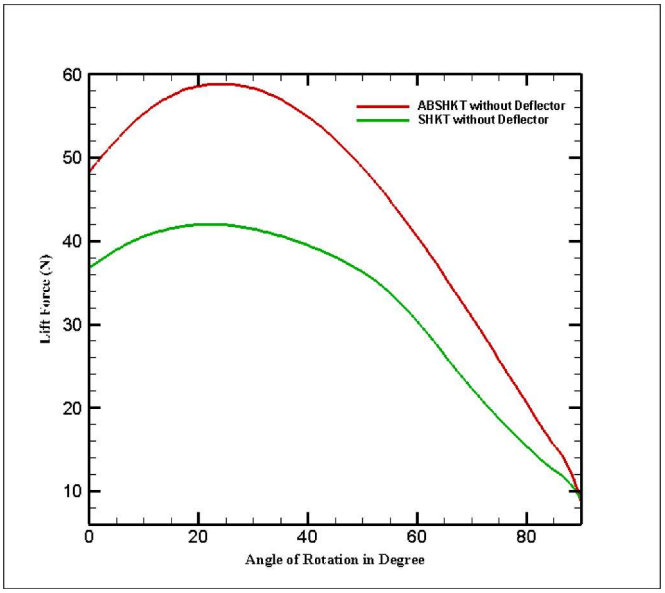

Fig. 9. Variation of lift force (N) about Angle of Rotation for the SHKT without Deflector and ABSHKT without Deflector.

with deflector the C_{tmax} and C_{pmax} are 0.357 and 0.25 at a TSR 0.7 and TSR 0.8 respectively, which is higher compared to the ABSHKT with deflector also tabulated in Table 3. The C_p of ABSHKT with deflector is 0.213 and the C_p of ABSHKT without deflector is 0.191 at TSR 1, which shows that the performance is improved with deflector implementation but the performance of ABSHKT with deflector is not higher compared to the SHKT with deflector. So, it is important to understand the flow physics around the various setup of turbines. The flow physics around the turbine is examined with pressure contour and velocity contour at the various angle of rotation 0°, 30°, 60°, 90°, 120° and 150° of the SHKT and ABSHKT with deflector.

5.1. *Changes of C_t concerning the rotational angle of the turbine*

Fig. 13 shows the changes of C_t concerning TSR for SHKT and ABSHKT without deflector and with deflector also, for 360° rotation of the turbine. The coefficient of torque C_t is altered, as positive and negative, for each degree of rotation. For SHKT with deflector, C_t increases in the range of 0° to 28° (and 181° to 208°) of rotation and reflects the highest value of 0.572 at 28° (and 208°) of rotation. Then the C_t is decrease in stages up to 124° (and 304°) degrees of rotation and then increases continuously up to 28° (and 208°) of rotation, with the lowest C_t = 0.04 observed at 124° (and 304°) rotation angle. For ABSHKT with deflector, C_t increases in the range of 0° to 40° (and 181° to 120°) of rotation and reflects the highest value of 0.695 at 40° (and 120°) of rotation. Then the C_t is decrease in stages up to 128° (and 308°) degrees of rotation and then increases continuously up to 40° (and 120°) of rotation, with the lowest C_t = -0.206 (negative) observed at 128° (and 308°) rotation angle. Fig. 13 shows the highest C_t of ABSHKT with deflector is higher compared to ABSHKT without deflector at a particular rotational angle, where the difference in the highest value of C_t is 0.093 and the lowest C_t of ABSHKT with deflector is lower compared to ABSHKT without deflector at a particular rotational angle, where the difference in the lowest value of C_t is 0.051. So, it is observed that, the ABSHKT with deflector has a higher average C_t compared to the ABSHKT without deflector but the average C_t of the ABSHKT with deflector is still lower compared to the SHKT with deflector. The C_t is negative in the range of 104° to 144° (and 284° to 324°) of rotation of ABSHKT with deflector, which is the significant reason for the lower performance of ABSHKT with deflector compare to SHKT with deflector. This is because of the high negative torque generated on the returning

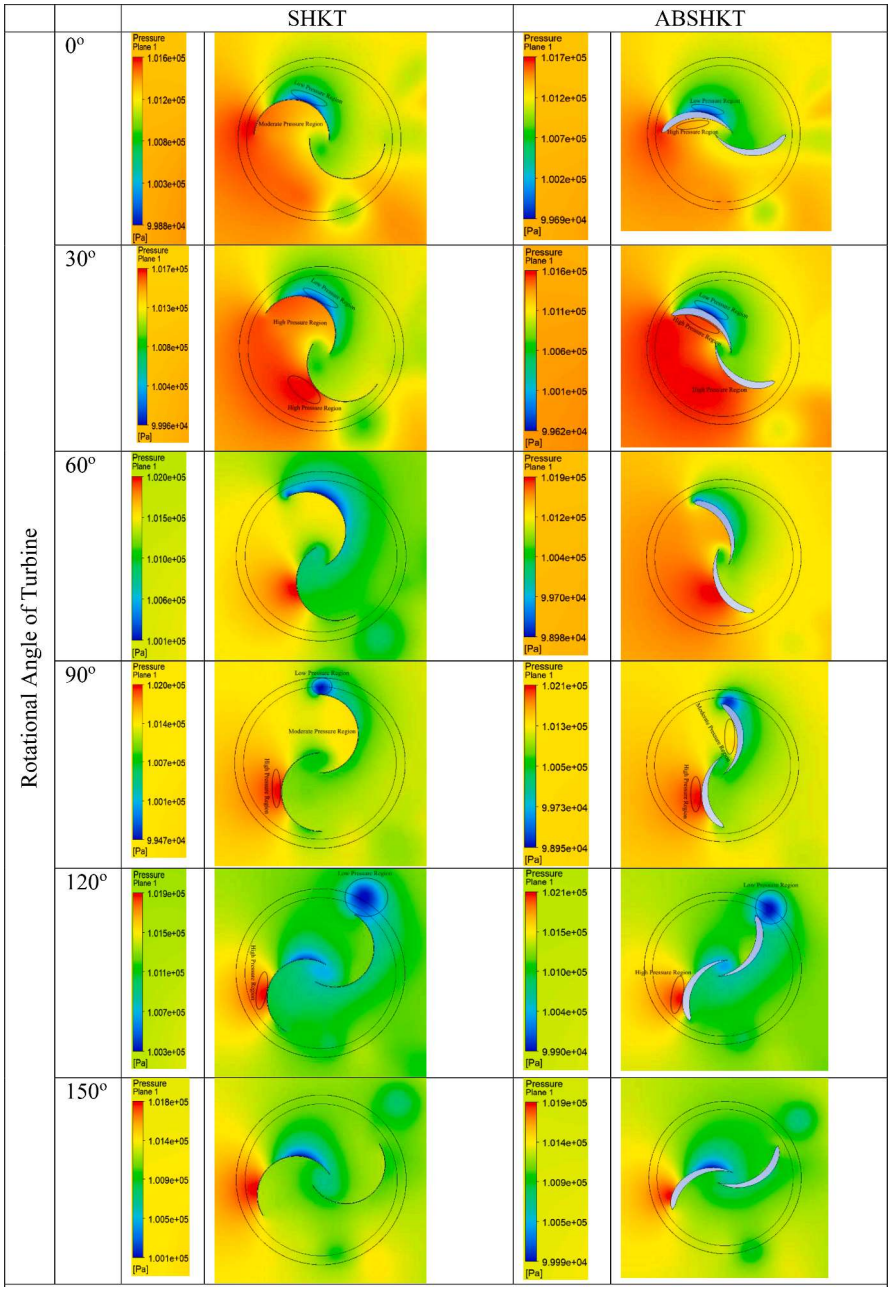

Fig. 10. Pressure Contour of SHKT and ABSHKT without Deflector.

blade of ABSHKT with deflector.

5.2. Changes of C_t and C_p about TSR

Fig. 11 shows the changes of C_t about TSR in the range of 0.7 to 1.1 and Fig. 12 shows the variation of C_p about TSR in the range of 0.7 to 1.1 for both the turbine with deflector. The coefficient of torque (C_t) is attained by averaging the C_t produced at all the rotational angles of 360°. And C_p significantly depends upon the value of C_t as per Eq. (3).

Fig. 11 shows that, the C_t is decreasing as the value of TSR increases for both turbines. This phenomenon was also observed in the previous investigation [6,11,12,17]. From the previous investigation [38], turbine angular velocity was reduced as the gradual load is employed on the turbine blades. The C_t achieves the highest value at TSR 0.7 for both SHKT and ABSHKT with deflector. The C_t achieves the value 0.357 for SHKT with deflector and ABSHKT with deflector achieves 0.324 at 0.7 TSR, which is almost 10% lower compare to SHKT with deflector.

Fig. 12 shows that, the value of C_p is moving upward up to some specific value of TSR then it is continuously decreasing as the TSR increases for both turbines. The C_p of SHKT with deflector is 0.249 at 0.7 TSR, which increases 0.25 at 0.8 TSR then it continuously decreases for the gradual TSR. And the C_p of ABSHKT with deflector is 0.227 at 0.7 TSR, which increases to 0.228 at 0.8 TSR then it continuously decreases for the gradual TSR.

5.3. Pressure contour

It is very important to analyze the flow field around the SHKT and ABSHKT with a deflector. As shown in Fig. 14, the pressure contours at various angles of rotation as 0°, 30°, 60°, 90°, 120° and 150°, are examined to analyze the flow field around both turbines with deflectors. The top view of both turbines is observed in Fig. 14, with the clockwise rotational direction of the turbine and the water current acting from the left side to the right side of the domain, and the high pressure is

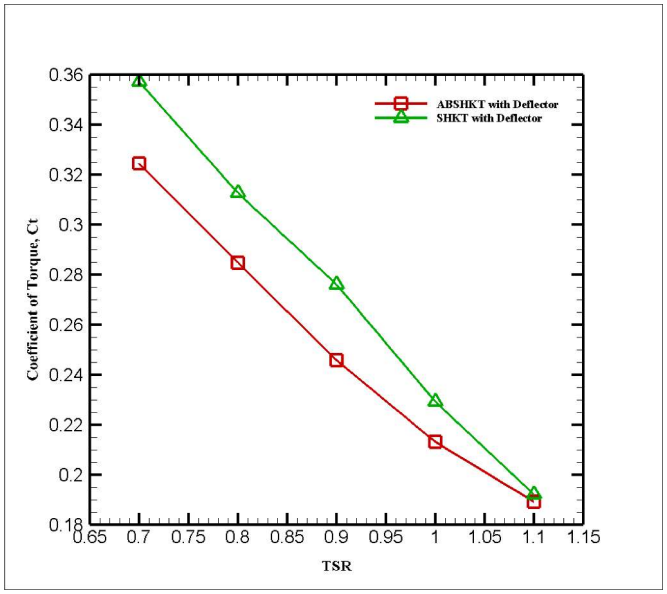

Fig. 11. Changes in Coefficient of Torque (C_t) about TSR for the SHKT with Deflector and ABSHKT with Deflector.

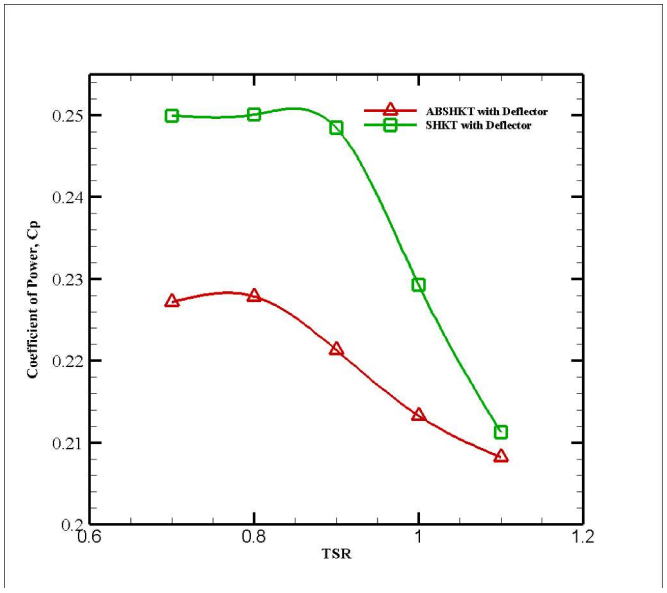

Fig. 12. Changes in Coefficient of Power (C_p) about TSR for the SHKT with Deflector and ABSHKT with Deflector.

Table 3
C_t and C_p value for SHKT and ABSHKT.

SHKT with Deflector				ABSHKT with Deflector			
C_{tmax}	TSR	C_{pmax}	TSR	C_{tmax}	TSR	C_{pmax}	TSR
0.357	0.8	0.25	0.8	0.324	0.7	0.227	0.8

represented by red color and low pressure is represented by blue color.

The pressure contours are offered with a high-pressure region generally at the concave side of the advancing blade and convex side of returning blade, a low-pressure region generally at the convex side of the advancing blade and concave side of returning blade. It is observed that, as the water current start, the high-pressure region is observed on the concave side of the advancing blade and the low-pressure region is observed on the convex side of the advancing blade and concave side of

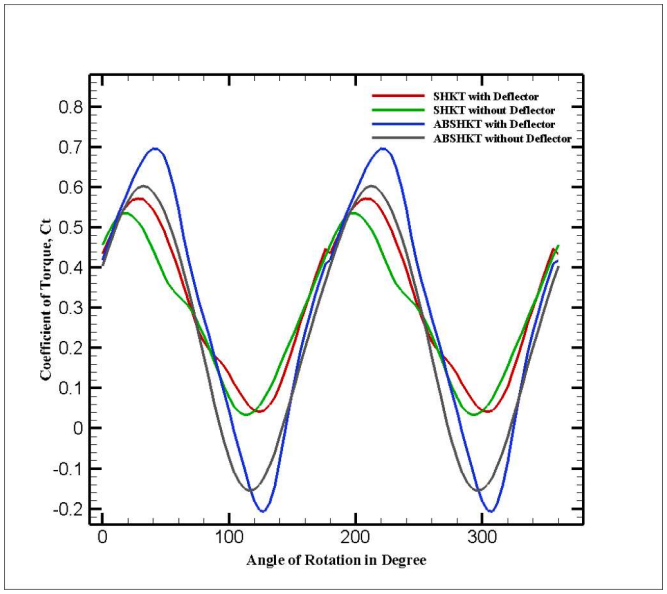

Fig. 13. Changes in Coefficient of Torque (C_t) about Angle of Rotation with TSR 0.9.

the returning bade, which created the pressure difference within the rotating zone and the turbine start to rotate. The phenomenon generates the power from the turbine which is extracted from the water current. As shown in Figs. 15 and 16 at the rotational angles 30° and 90° for both the turbine, by the implementation of a deflector plate, the pressure generated on the convex side of the returning blade decreases compared to the turbine without the deflector because of that the performance of the turbine with a deflector has greater performance compared to the turbine without deflector. This phenomenon is observed in both SHKT and ABSHKT.

For SHKT with deflector has pressure difference on the advancing blade is 1715pascal and for returning blade 1129pascal at a rotational angle of 30°, because of this pressure difference positive torque is generated at the SHKT.

The same phenomenon for ABSHKT with deflector plate has pressure difference on advancing blade is 2316pascal and for returning blade 738pascal at the rotational angle 30°, because this pressure difference positive torque is generated at the ABSHKT. At the rotational angle of 30°, higher torque is generated for ABSHKT with deflector compared to SHKT with deflector, because lift force is generated for the particular angle of ABSHKT with deflector as shown in Fig. 9. But for the rotational angles 90° and 120° (Figs. 15 and 16), the flow diverted by the deflector plate effect more to the SHKT with deflector compare to the ABSHKT with deflector. At a particular rotational angle, the convex surface of the returning blade of SHKT is closer to the deflector plate, because of the circular shape of SHKT's blade, compared to the convex surface of the returning blade of ABSHKT because the airfoil shape of ABSHKT's blade. Because of that, the center of pressure generated on the returning blade of SHKT with deflector is closer to the center of the turbine compared to the center of pressure generated on the returning blade of ABSHKT with deflector, so the torque arm generated on the convex side of the returning blade of ABSHKT with deflector is longer compare to the SHKT with deflector. So it is observed that, the negative torque generation on the convex side of the returning blade of ABSHKT with deflector is higher compared to the negative torque generation on the convex side of the returning blade of SHKT with deflector. Because of these phenomena, the overall performance of ABSHKT with a deflector has lower performance compared to the SHKT with a deflector.

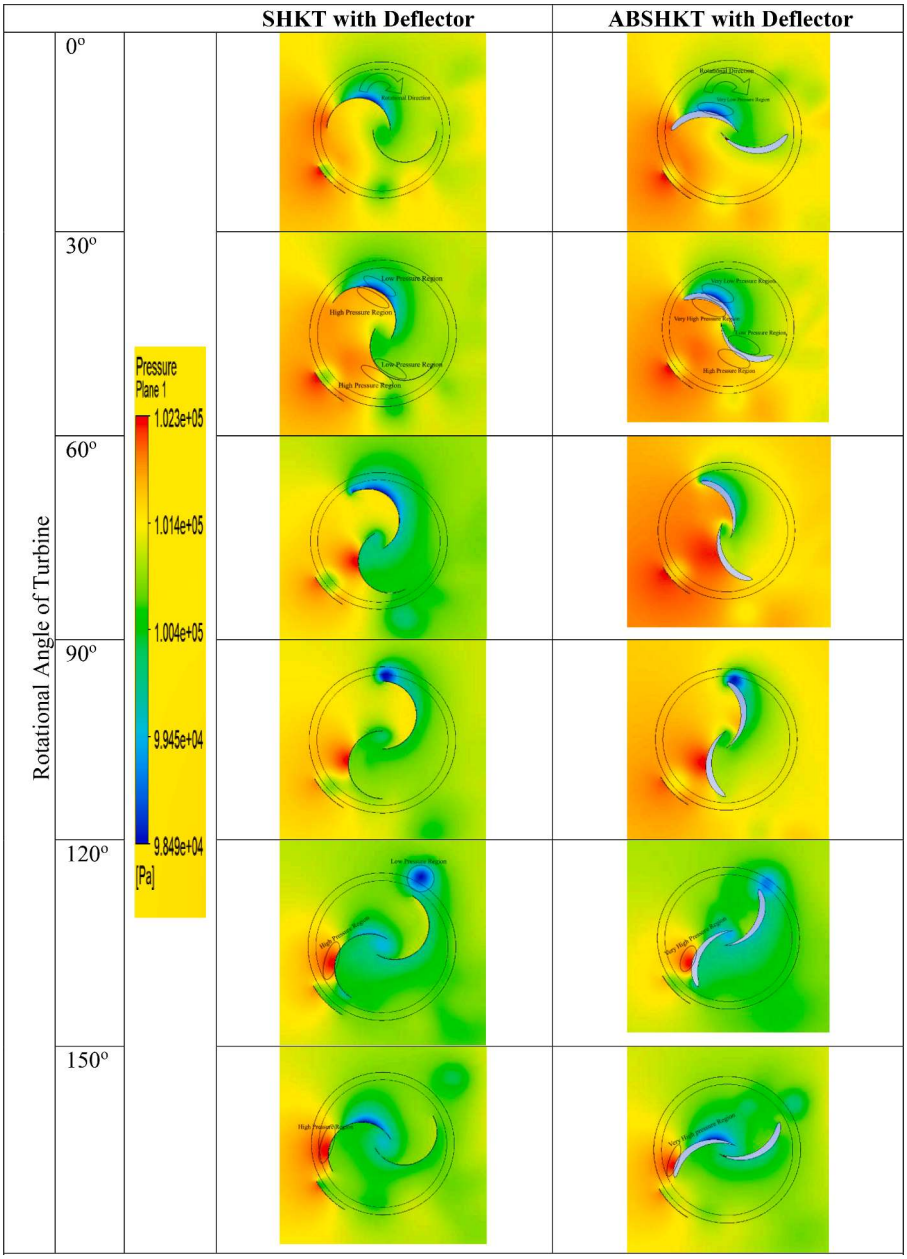

Fig. 14. Pressure Contour of SHKT and ABSHKT with Deflector.

5.4. Velocity contour

As shown in Fig. 17, the velocity contour is presented for the SHKT and ABSHKT with deflector at rotational angles 0°, 30°, 60°, 90°, 120° and 150° with the inlet velocity water current 1 m/s. This velocity contour presents the velocity distribution at the different regions of the rotating and stationary domains. The top view of both turbines is observed in Fig. 17, with the clockwise rotational direction of the turbine and the water current acting from the left side to the right side of the domain, and the high velocity is represented by red color and low velocity is denoted by blue color. At the 90° of a rotational angle, the high-velocity region is generated at the tip of the advancing blade, which is responsible for less momentum transfer from the water current to the turbine. The low pressure and wake region are generated on the downstream side of both turbines at the entire rotational angle of a turbine, which is also observed in the former study [6,11,12,17]. It is also observed that, the advancing blade of the ABSHKT with deflector experience a lower velocity gradient compare to the SHKT with deflector. Also, less quantity of water is enclosed inside the blades of ABSHKT with deflector compared to SHKT with deflector. This phenomenon of ABSHKT with deflector generates less torque and consequently less C_p compared to SHKT with deflector.

At 120° of rotational angle, the high-velocity region is observed at both the tip of the returning blade of ABSHKT with deflector, which is not observed for the SHKT with deflector. These strengthened velocity vectors are moving from the returning blade, which is responsible for the decline of the performance of ABSHKT compared to SHKT with a deflector.

6. Conclusion

In the present investigation, a newly Airfoil Bladed Savonius Hydrokinetic Turbine (ABSHKT) is proposed with a deflector plate and its performance is compared with the conventional semi-circular Savonius Hydrokinetic Turbine (SHKT) with a deflector plate. The former investigations [5,27] and [28] are conducted on the implementation of a

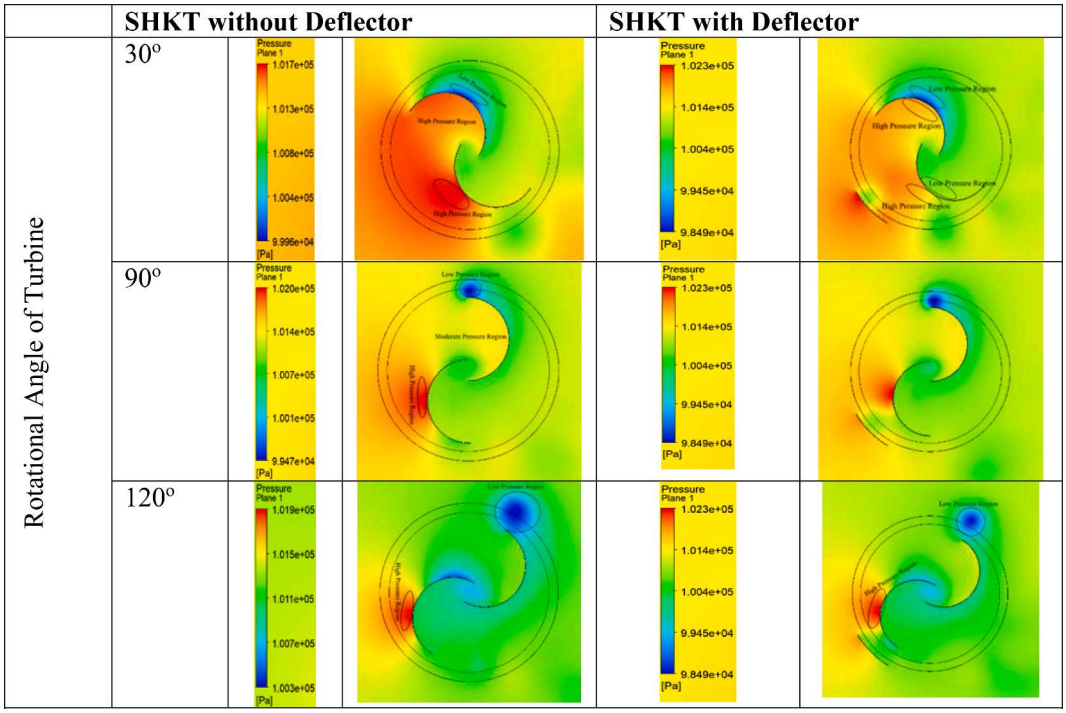

Fig. 15. Comparison of Pressure Contour for SHKT without Deflector and SHKT with Deflecto.

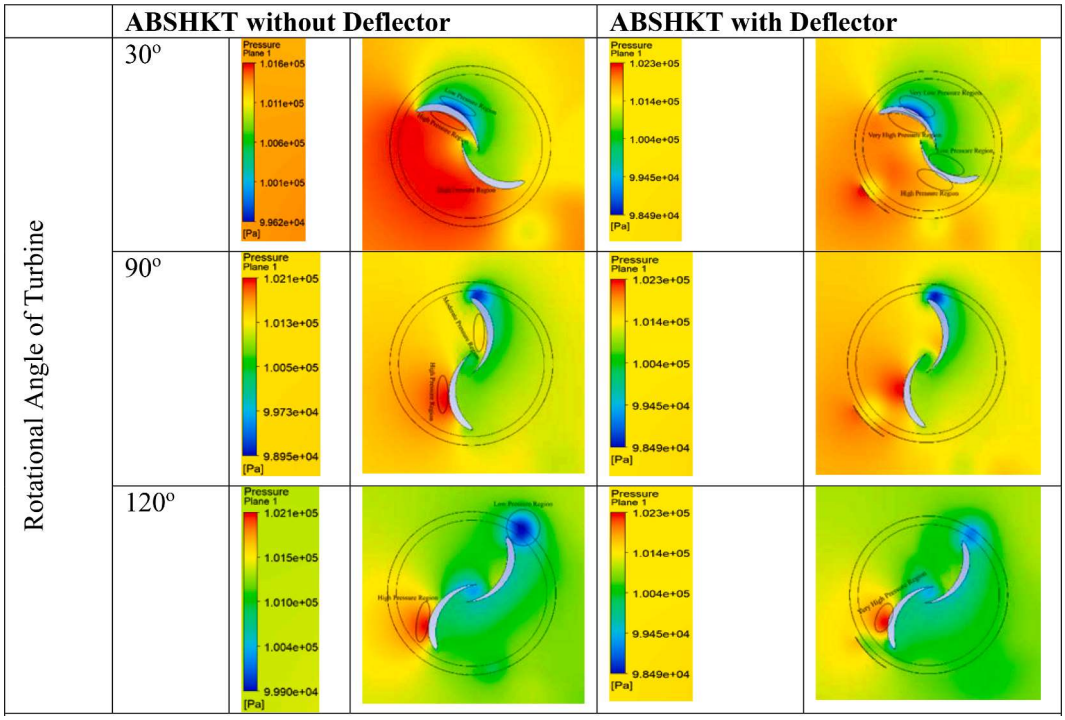

Fig. 16. Comparison of Pressure Contour for ABSHKT without Deflector and ABSHKT with Deflector.

section of airfoil blades only but the present investigation is conducted to analyze the performance of full NACA6409 9% airfoil blades in place of conventional semi-circular blades of a turbine. The CFD simulation, with ANSYS-CFX 2020R, is carried out to analyze the performance of both turbines. On the base of the result and discussion, the following conclusions are established.

- The overall performance of the ABSHKT is lower than the SHKT.
- For some degree of rotational angle, ABSHKT generates higher torque than SHKT, so a deflector plate is implemented to improve performance.
- The performance of ABSHKT with a deflector is higher compared to ABSHKT without a deflector, but the performance of ABSHKT with a deflector is lower compared to SHKT with a deflector.
- The value of C_{tmax} and C_{pmax} of the SHKT with deflector is 0.357 at 0.8 TSR and 0.25 at 0.8 TSR respectively.

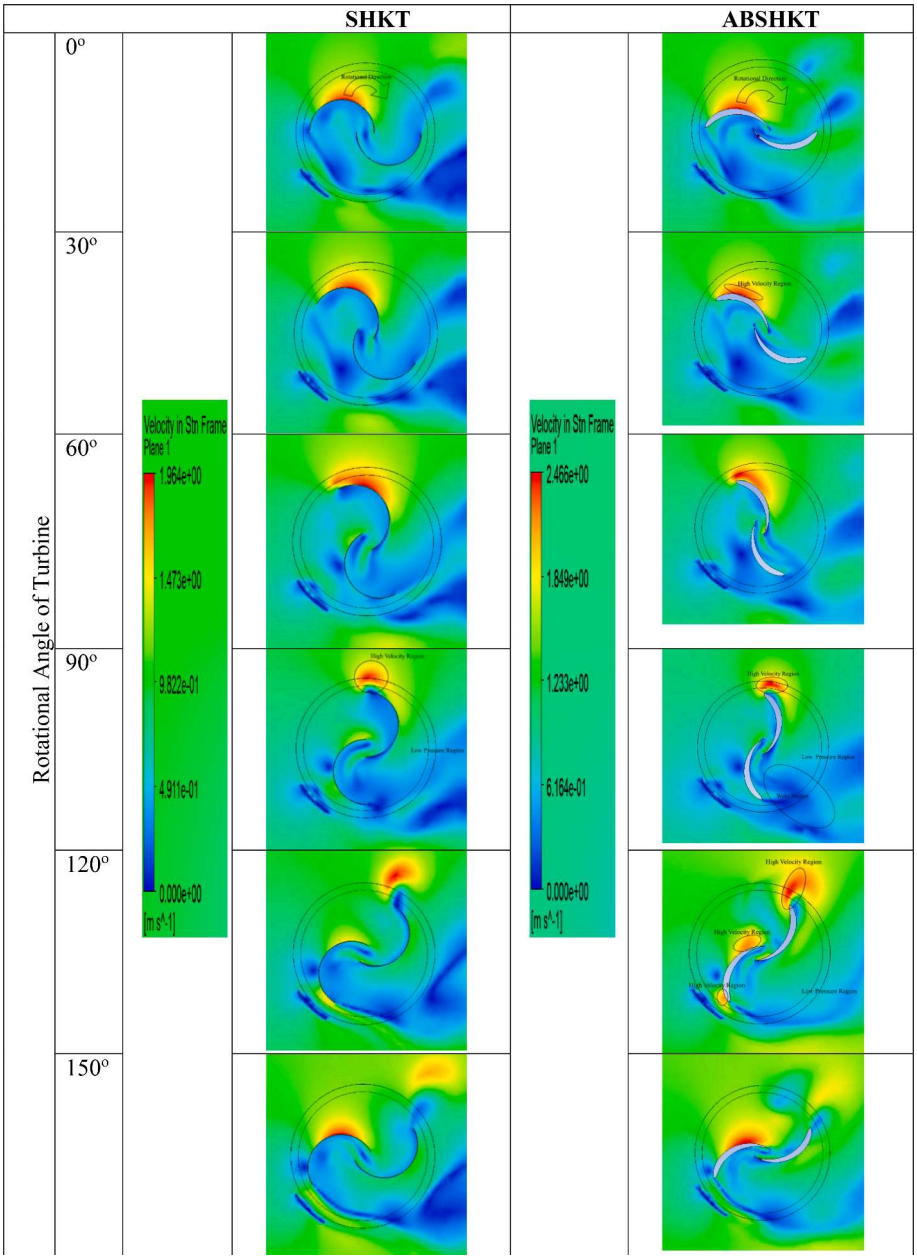

Fig. 17. Velocity Contour of SHKT and ABSHKT with Deflector.

- The value of C_{tmax} and C_{pmax} of the ABSHKT with deflector is 0.324 at 0.7 TSR and 0.227 at 0.8 TSR respectively.
- The less quantity of water is enclosed inside the blades of ABSHKT with deflector compared to SHKT with deflector, so a loss of hydrokinetic energy of water current by ABSHKT with deflector.
- At 120° of rotational angle, the high-velocity region is observed at both the tip of the returning blade of ABSHKT with deflector, which is responsible for the decline of the performance of ABSHKT compared to SHKT with deflector.
- It is suggested that, diversion of the flow from returning blade by implementing an enhanced augmentation technique can improve the performance of ABSHKT.

Declaration of Competing Interest

The authors declare that they have no known competing financial interests or personal relationships that could have appeared to influence the work reported in this paper.

Data availability

Data will be made available on request.

References

[1] Bp Statistical Review of World Energy, 2022, Available from: (https://www.bp.com/en/global/corporate/energy-economics/statistical-review-of-world-energy.html).
[2] Global Energy Review 2020 by IEA. Available from: (https://www.iea.org/reports/global-energy-review-2020).
[3] I. Kougias, G. Aggidis, F. Avellan, S. Deniz, U. Lundin, A. Moro, S. Muntean, D. Novara, J.I. Pérez-Díaz, E. Quaranta, P. Schild, N. Theodossiou, Analysis of emerging technologies in the hydropower sector, in: Renewable and Sustainable Energy Reviews, 113, Elsevier Ltd, 2019, https://doi.org/10.1016/j.rser.2019.109257.
[4] J. Xu, T. Ni, B. Zheng, Hydropower development trends from a technological paradigm perspective, Energy Convers. Manage. 90 (2015) 195–206, https://doi.org/10.1016/j.enconman.2014.11.016.

[5] M. Basumatary, A. Biswas, R.D. Misra, CFD analysis of an innovative combined lift and drag (CLD) based modified Savonius water turbine, Energy Convers. Manage. 174 (2018) 72–87, https://doi.org/10.1016/j.enconman.2018.08.025.
[6] A. Kumar, R.P. Saini, Performance analysis of a single stage modified Savonius hydrokinetic turbine having twisted blades, Renew Energy 113 (2017) 461–478, https://doi.org/10.1016/j.renene.2017.06.020.
[7] N.R. Maldar, C.Y. Ng, E. Oguz, A review of the optimization studies for Savonius turbine considering hydrokinetic applications, in: Energy Conversion and Management, 226, Elsevier Ltd, 2020, https://doi.org/10.1016/j.enconman.2020.113495.
[8] M.A. Kamoji, S.B. Kedare, S.v. Prabhu, Experimental investigations on single stage, two stage and three stage conventional Savonius rotor, International Journal of Energy Research 32 (10) (2008) 877–895, https://doi.org/10.1002/er.1399.
[9] K.S. Jeon, J.I. Jeong, J.K. Pan, K.W. Ryu, Effects of end plates with various shapes and sizes on helical Savonius wind turbines, Renew. Energy 79 (1) (2015) 167–176, https://doi.org/10.1016/j.renene.2014.11.035.
[10] H.J. Vermaak, K. Kusakana, S.P. Koko, Status of micro-hydrokinetic river technology in rural applications: a review of literature, Renewable and Sustainable Energy Reviews 29 (2014) 625–633, https://doi.org/10.1016/j.rser.2013.08.066.
[11] R. Alipour, R. Alipour, F. Fardian, S.S.R. Koloor, M. Petrů, Performance improvement of a new proposed Savonius hydrokinetic turbine: a numerical investigation, Energy Reports 6 (2020) 3051–3066, https://doi.org/10.1016/j.egyr.2020.10.072.
[12] P.K. Talukdar, A. Sardar, V. Kulkarni, U.K. Saha, Parametric analysis of model Savonius hydrokinetic turbines through experimental and computational investigations, Energy Convers. Manage. 158 (2018) 36–49, https://doi.org/10.1016/j.enconman.2017.12.011.
[13] S. Singha, R.P. Saini, Performance analysis of a modified savonius hydrokinetic turbine, Springer Proc. Mathem. Statistics 308 (2020) 377–392, https://doi.org/10.1007/978-981-15-1338-1_28.
[14] Seliger, G. 1947-, CIRP - The International Academy for Production Engineering, Technische Universität Berlin Institut für Werkzeugmaschinen und Fabrikbetrieb, Global Conference on Sustainable Manufacturing 11 2013.09.23-25 Berlin, & GCSM 11 2013.09.23-25 Berlin. (2013). Proceedings /11th Global Conference on Sustainable Manufacturing innovative solutions ; Berlin, Germany, 23rd - 25th September 2013 ; proceedings. Univ.-Verl. der TU.
[15] M. Mosbahi, S. Elgasri, M. Lajnef, B. Mosbahi, Z. Driss, Performance enhancement of a twisted Savonius hydrokinetic turbine with an upstream deflector, Int. J. Green Energy 18 (1) (2021) 51–65, https://doi.org/10.1080/15435075.2020.1825444.
[16] Y. Zhang, C. Kang, Y. Ji, Q. Li, Experimental and numerical investigation of flow patterns and performance of a modified Savonius hydrokinetic rotor, Renew. Energy 141 (2019) 1067–1079, https://doi.org/10.1016/j.renene.2019.04.071.
[17] C.M. Shashikumar, H. Vijaykumar, M. Vasudeva, Numerical investigation of conventional and tapered Savonius hydrokinetic turbines for low-velocity hydropower application in an irrigation channel, Sustain. Energy Technol. Assess. 43 (2021), https://doi.org/10.1016/j.seta.2020.100871.
[18] Patel, V.K., Shah, K., & Rathod, V. (2021). Performance enhancement of Savonius hydrokinetic turbine with a unique vane shape: an experimental investigation (pp. 1453–1463). https://doi.org/10.1007/978-981-15-5955-6_138.
[19] Prabowoputra, D.M., Hadi, S., Prabowo, A.R., & Sohn, J.M. (2020). Performance investigation of the savonius horizontal water turbine accounting for stage rotor design.
[20] A. Kumar, R.P. Saini, G. Saini, G. Dwivedi, Effect of number of stages on the performance characteristics of modified Savonius hydrokinetic turbine, Ocean Eng. (2020) 217, https://doi.org/10.1016/j.oceaneng.2020.108090.
[21] V. Patel, G. Bhat, T.I. Eldho, S.v. Prabhu, Influence of overlap ratio and aspect ratio on the performance of Savonius hydrokinetic turbine, Int. J. Energy Res. 41 (6) (2017) 829–844, https://doi.org/10.1002/er.3670.
[22] H. Alizadeh, M.H. Jahangir, R. Ghasempour, CFD-based improvement of Savonius type hydrokinetic turbine using optimized barrier at the low-speed flows, Ocean Eng. 202 (2020), https://doi.org/10.1016/j.oceaneng.2020.107178.
[23] K. Golecha, T.I. Eldho, S.v. Prabhu, Influence of the deflector plate on the performance of modified Savonius water turbine, Appl. Energy 88 (9) (2011) 3207–3217, https://doi.org/10.1016/j.apenergy.2011.03.025.
[24] B. Wahyudi, S. Adiwidodo, The influence of moving deflector angle to positive torque on the hydrokinetic cross flow savonius vertical axis turbine, Int. Energy J. 17 (2017) (2017) 11–22.
[25] E. Kerikous, D. Thévenin, Optimal shape and position of a thick deflector plate in front of a hydraulic Savonius turbine, Energy 189 (2019), https://doi.org/10.1016/j.energy.2019.116157.
[26] N. Thakur, A. Biswas, Y. Kumar, M. Basumatary, CFD analysis of performance improvement of the Savonius water turbine by using an impinging jet duct design, Chin. J. Chem. Eng. 27 (4) (2019) 794–801, https://doi.org/10.1016/j.cjche.2018.11.014.
[27] M. Basumatary, A. Biswas, R.D. Misra, Experimental verification of improved performance of Savonius turbine with a combined lift and drag based blade profile for ultra-low head river application, Sustain. Energy Technol. Assess. 44 (2021), https://doi.org/10.1016/j.seta.2021.100999.
[28] Z.U. Khan, Z. Ali, E. Uddin, Performance enhancement of vertical axis hydrokinetic turbine using novel blade profile, Renew. Energy 188 (2022) 801–818, https://doi.org/10.1016/j.renene.2022.02.050.
[29] Gerakopulos, R., Boutilier, M.S.H., & Yarusevych, S. (2010). Aerodynamic characterization of a NACA 0018 airfoil at low Reynolds numbers.
[30] M.F. Ismail, K. Vijayaraghavan, The effects of aerofoil profile modification on a vertical axis wind turbine performance, Energy 80 (2015) 20–31, https://doi.org/10.1016/j.energy.2014.11.034.
[31] M.H. Mohamed, Performance investigation of H-rotor Darrieus turbine with new airfoil shapes, Energy 47 (1) (2012) 522–530, https://doi.org/10.1016/j.energy.2012.08.044.
[32] W. Tian, B. Song, J.H. van Zwieten, P. Pyakurel, Computational fluid dynamics prediction of a modified savonius wind turbine with novel blade shapes, Energies 8 (8) (2015) 7915–7929, https://doi.org/10.3390/en8087915.
[33] N. Kolekar, A. Banerjee, Performance characterization and placement of a marine hydrokinetic turbine in a tidal channel under boundary proximity and blockage effects, Appl. Energy 148 (2015) 121–133, https://doi.org/10.1016/j.apenergy.2015.03.052.
[34] N.K. Sarma, A. Biswas, R.D. Misra, Experimental and computational evaluation of Savonius hydrokinetic turbine for low-velocity condition with comparison to Savonius wind turbine at the same input power, Energy Convers. Manage. 83 (2014) 88–98, https://doi.org/10.1016/j.enconman.2014.03.070.
[35] S. Roy, A. Ducoin, Unsteady analysis on the instantaneous forces and moment arms acting on a novel Savonius-style wind turbine, Energy Convers. Manage. 121 (2016) 281–296, https://doi.org/10.1016/j.enconman.2016.05.044.
[36] F.R. Menter, Two-equation eddy-viscosity turbulence models for engineering applications, AIAA J. 32 (8) (1994) 1598–1605, https://doi.org/10.2514/3.12149.
[37] R. Lanzafame, S. Mauro, M. Messina, Wind turbine CFD modeling using a correlation-based transitional model, Renew. Energy 52 (2013) 31–39, https://doi.org/10.1016/j.renene.2012.10.007.
[38] S. Roy, U.K. Saha, Wind tunnel experiments of a newly developed two-bladed Savonius-style wind turbine, Appl. Energy 137 (2015) 117–125, https://doi.org/10.1016/j.apenergy.2014.10.022.